African Journal of Physical Science, Volume 4, Number 1, 2011

A COMPUTATION OF LAMINAR FLOW IN OPEN CHANNELS AND ITS APPLICATION TO SHEET EROSION

J. A. Adegoke, and G. B. Egbeyale
Department of Physics
University of Ibadan, Oyo State, Nigeria

ABSTRACT

The results of an investigation of open channel flow in the laminar and transition range are presented. This type of flow found its application in runoff from rainfall. Values of Reynolds number were determined for different slopes in the range $1^0 \leq \theta \leq 45^0$. It was found that the velocity of the fluid increases as the slope of the bottom surface increases. There was a point where the laminar flow range change drastically to transitional flow range and later turbulent.
Keywords: Viscosity, Velocity, Laminar flow, Transitional flow, Reynolds number and Turbulent flow.

INTRODUCTION

The data that form the basis of this paper were simulated as part of an investigation of laminar flow in open channels. It is expected that the results of the study will be more useful to engineers because it founds its application in sheet erosion. This investigation was undertaken to obtain a better understanding of the sheet flow produced by water erosion during rainfall. In laminar flow, agitation of fluid particle is of molecular nature only, and these particles are constrained to motion in essentially paralleled paths by the action of viscosity (Vennard, 1947). Viscosity of a fluid is a measure of how large a stress is required to produce unit shear rate. The effect of viscosity causes the flow of a fluid to occur under two very different conditions; laminar flow and turbulent flow. Hagen first published the law of laminar flow in pipes of circular section in 1839 and by Poiseuille in 1840, (Streeter and Wylie, 1983). From experimental results and was derived analytically by Wiederman. Boussinesq (1868) derived the equation of laminar flow in a pipe of rectangular section of any ratio of width to depth. A much simpler derivation of this equation was presented by Horton, Leuch and Vliet (1934). It was proved correct by experiments but lack of adequate data on flow on surfaces leave the question of the legality of the equation unresolved. It is the purpose of this paper to present series of data to investigate variable flow in open channel. The earliest researches on this subject were Hopt (1910), Jeffreys (1925). They all carried out experiment work. Chow (1959) also indicated that the experimental data in open channels of both smooth and rough surfaces showed the same general relationship between f_c and N_R as in the pipe flow. Owen's (1954) results on surfaces of polished brass checked very well with the theoretical values for retangular channel.

MATERIALS AND METHOD

For laminar flow in rectangular pipes having a width *b* and depth of *2Y* was first derived analytically by Boussinesq (1868) and was given as;

$$v = -\frac{Y^2}{2\mu}\frac{dp}{dz}\left[1-\frac{y^2}{Y^2}-\frac{32}{\pi^3}\sum_{n=0}\frac{(-1)^n}{(2n+1)^2}\frac{\cosh\frac{2n+1}{2}\frac{\pi x}{Y}}{\frac{2n+1}{4}\frac{\pi b}{Y}}\cos\frac{2n+1}{2}\frac{\pi y}{Y}\right] \qquad 1$$

In which *x* and *y* are the coordinates with respect to the center of the pipe of a point where the velocity is *v*. By substituting gSo/v for $-(1/\mu)dp/dz$, equation 1 becomes

$$v = \frac{gS_oY^2}{2v}\left[1-\frac{y^2}{Y^2}-\frac{32}{\pi^3}\sum_{n=0}^{\infty}\frac{(-1)^n}{(2n+1)^3}\frac{\cosh\frac{2n+1}{2}\frac{\pi x}{Y}}{\frac{2n+1}{4}\frac{\pi b}{Y}}\cos\frac{2n+1}{2}\frac{\pi y}{Y}\right] \qquad 2$$

Where; S_0 = Slope of Bottom Surface,
v = velocity at any distance y
y = vertical distance from water surface

Y =water depth
v = kinematic viscosity
g = gravitational acceleration

Because the flow pattern in a rectangular pipe is symmetrical about the horizontal centre line, equation (2) can be applied to a rectangular channel of width *b* and depth *Y* to obtain the following expression for average velocity.

$$v = \frac{gS_oY^2}{3v}\left[1 - \frac{384}{\pi^5}\frac{Y}{b}\sum_{n=0}^{\infty}\frac{1}{(2n+1)^5}\cdot\tanh\frac{2n+1}{4}\frac{\pi b}{Y}\right] \quad 3$$

Considering a laminar flow based on the equilibrium between the component of weight, in the direction of flow, and the shearing resistance of the channel bottom is derived analytically by Horton et al., (1934).
The equation for velocity at any distance y from the channel bottom is given as

$$v = \frac{gSo}{v}\left(Yy - y^2\right) \quad 4$$

When zero shearing stress at the free water surface was assumed.
For infinite width, *Y/b* = 0.
Therefore equation (3) becomes

$$V = \frac{gS_oY^2}{3v} \quad 5$$

Rearranging equation (5), we have

$$S_o = \frac{3Vv}{gY^2} \quad 6$$

If Reynolds number in the open channel is given as

$$N_R = \frac{VY}{v} \quad 7$$

Where N_R = Reynolds number
V = mean velocity
Equation (6) can be rearranged as

$$S_o = \frac{6v\cdot 1\cdot v^2}{VY\cdot Y\cdot 2g}$$

$$S_o = \frac{6}{N_R}\frac{1}{Y}\frac{v^2}{2g} \quad 8$$

By replacing $6/N_R$ with f_c,

$$S_o = f_c\frac{1}{Y}\frac{V^2}{2g} \quad 9$$

Where f_c = Coefficient of Friction
This equation corresponds to the general energy loss formula for pipe flow.

DISCUSSION

Table 1 in the appendix shows generated data for vertical distance from bottom surface and velocity components in the direction of flow at different slope range $1^0 \leq \theta \leq 45^0$ Fig. 1 shows a sample curve for the relationship between vertical distance from bottom surface and the velocity component in the direction of flow at S_0 = 0.017. From the graph, it was noted that at about 0.45cm from the bottom of the water upward, the shear stress is virtually constant for a particular value of S_0 thus velocity remain constant at a "skin depth" of 20000m/s, 42,000m/s, 63,000m/s, 85,000m/s, 105,000m/s, 440,000m/s, 566,000m/s, 700,000m/s, 850,000, 1020,000m/s, 1210,000m/s from the water-air boundary at S_0 = 0.017, 0.035, 0.052, 0.07, 0.087, 0.36, 0.466, 0.577, 0.7, 0.839 and 1.000 respectively. At *y* = *Y* (water surface), velocity gradient, *(du/dy)* = 0. Therefore shear stress is equal to zero at the surface. In addition, the inverse of slope in fig 1 can be used to find the shearing stress τ along the velocity profile. It should be noted that stress, τ is directly proportional to velocity gradient *du/dy*. Fig 2 shows a linear graphical relationship between vertical distance from surface and velocity component in the direction of flow at different slopes. It was found that at low velocities the particles in the open channel moved in parallel layers. As the velocity increases the laminar flow broke down into transition or turbulent flow at N_R>440. The velocity at which these particles of the fluid change momentarily is regarded as critical velocity. Considering the motion of fluid along the solid boundary, observation shows that there is no velocity at the boundary and that velocity increases with increasing distance from the boundary to the air-water surface. This velocity also increases as the slope of the bottom channel increases. These results are in line with the Chezy –manning equation. Reynolds number was computed. The results obtained are N_R = 213.88, 440.346, 1094.57 and 4529.10 at different slopes 0.017,0.035,0.087 and 0.36 respectively. It shows that the flow is laminar when S_o<0.087 at y = 0.15 and change to transition range as $S_o \geq$ 0.087 .For larger values of Reynolds number flow is in a transition range in which it is quite common to have values of friction coefficient increase as Reynolds number increases .For range of N_R greater than those in the transition range, flow becomes fully turbulent and the typical reduction of friction coefficient values begins. The concept of specific energy is helpful in the explanation and analysis of some problems of open channel .The data show that an increase in depth is seen to cause an increase in specific energy in sub critical flow but a decrease in specific energy in supercritical flow. In other words, specific energy may be gained or lost depending on whether the depths of flow are greater or less than critical depth.

CONCLUSION

The data presented will be of value in determining the characteristics of flow in sheet erosion. The results show that there is linear relationship between slope and velocity and the extend of this was determined. It also showed parabolic properties of the velocity profile that can be used to get the mean velocity and the shearing stress, which in turn helps to determine the severity of eroded solid particles. The shearing stress of laminar flow was also shown to produce velocity distributions characterized by reduced velocity near the boundary surfaces. By calculation, the friction coefficient f_c was determined from the relationship in equation (9) which is a major determinant of the type of flow (Laminar or Turbulent) vis-à-vis the magnitude of solid particles erosion. The information obtained from this simulation also can be applied in venturi flume, which in turn can be used in water irrigation.

REFERENCES

Boussinesq, M .J.(1868): Memoire sur L influence des frottamenta dans les monvements reguliers des fluids J. Math pures el appl, serie ii,xii,277-424.

Chow V.T. ,Open chanelHydraulics ,McGraw-Hill Book Co. 1959

Hopf, L . (1910):Turbulenz bei einem flusse Ann. Physik, 337 Vierte Folge, 32,777-808.

Horton R.E, Leach H.R. and Van Vliet R. (1934) :Laminar sheet flow, Trans. Am. Geophy. Union, part (ii) 393-404.

Jeffreys, H.(1925) : The flow of water in an inclined channel of rectangular section; phil. Mag. 6th series, 40.293, 793-807.

Owen, W.M, (1954): Laminar to Turbulent flow in a wide open channel Trans.Am.Soc.Civil Engrs.,119, 1157-1164.

Strecter L.V. and Wylie E.B! 91983). Fluid Mechanic. New York Mc-Graw-Hill.

Vennard J.K.(1947) :Elementary fluid mechanics, John Wiley and sons. Inc.U.S.A. Troppan company, Ltd. Japan.

APPENDIX

Table 1: Velocity of flow at different slopes and at different vertical distance from water surface.

	so=0.017	So=0.035	so=0.052	so=0.070	so=0.087	so=0.364	so=0.466	so=0.577	so=0.700	so=0.839	so=1.000
y	V1	V2	v3	v4	v5	v6	v7	v8	v9	v10	v11
0.005	414.8404	853.2125	1267.63	1706.425	2120.843	8873.41	11379.42	14065.82	17064.25	20452.72	24377.5
0.01	825.5115	1697.85	2522.52	3395.7	4220.37	17657.64	22644.47	27990.27	33957	40699.89	48510
0.015	1232.013	2533.913	3764.67	5067.825	6298.583	26352.69	33795.15	41773.36	50678.25	60741.5	72397.5
0.02	1634.346	3361.4	4994.08	6722.8	8355.48	34958.56	44831.47	55415.08	67228	80577.56	96040
0.025	2032.509	4180.313	6210.75	8360.625	10391,06	43475.25	55753.43	68915.44	83606.25	100208.1	119437.5
0.03	2426.504	4990.65	7414.68	9981.3	12405.33	51902.76	66561.01	82274.43	99813	119633	142590
0.035	2816.328	5792.413	8605.87	11584.83	14398.28	60241.09	77254.23	95492.06	115848.3	138852.4	165497.5
0.04	3201.984	6585.6	9784.32	13171.2	16369.92	68490.24	87833.09	108568.3	131712	157866.2	188160
0.045	3583.47	7370.213	10950.03	14740.43	18320.24	76650.21	98297.58	121503.2	147404.3	176674.5	210577.5
0.05	3960.788	8146.25	12103	16292.5	20249.25	84721	108647.7	134296.8	162925	195277.3	232750
0.055	4333.935	8913.713	13243.23	17827.43	22156.94	92702.61	118883.5	146948.9	178274.3	213674.4	254677.5
0.06	4702.914	9672.6	14370.72	19345.2	24043.32	100595	129004.8	159459.7	193452	231866	276360
0.065	5067.723	10422.91	15485.47	20845.83	25908.38	108398.3	139011.9	171829.2	208458.3	249852.1	297797.5
0.07	5428.364	11164.65	16587.48	22329.3	27752.13	116112.4	148904.5	184057.2	223293	267632.6	318990

0.075	5784.834	11897.81	17676.75	23795.63	29574.56	123737.3	158682.8	196143.9	237956.3	285207.6	339937.5
0.08	6137.136	12622.4	18753.28	25244.8	31375.68	131273	168346.8	208089.3	252448	302577	360640
0.085	6485.268	13338.41	19817.07	26676.83	33155.48	138719.5	177896.3	219893.3	266768.3	319740.8	381097.5
0.09	6829.232	14045.85	20868.12	28091.7	34913.97	146076.8	187331.5	231555.9	280917	336699.1	401310
0.095	7169.025	14744.71	21906.43	29489.43	36651.14	153345	196652.3	243077.1	294894.3	353451.8	421277.5
0.1	7504.65	15435	22932	30870	38367	160524	205858.8	254457	308700	369999	441000
0.105	7836.105	16116.71	23944.83	32233.43	40061.54	167613.8	214950.9	265695.5	322334.3	386340.6	460477.5
0.11	8163.392	16789.85	24944.92	33579.7	41734.77	174614.4	223928.6	276792.7	335797	402476.7	479710
0.115	8486.508	17454.41	25932.27	34908.83	43386.68	181525.9	232792	287748.5	349088.3	418407.2	498697.5
0.12	8805.456	18110.4	26906.88	36220.8	45017.28	188348.2	241541	298562.9	362208	434132.2	517440
0.125	9120.234	18757.81	27868.75	37515.63	46626.56	195081.3	250175.6	309235.9	375156.3	449651.6	535937.5
0.13	9430.844	19396.65	28817.88	38793.3	48214.53	201725.2	258695.9	319767.6	387933	464965.4	554190
0.135	9737.283	20026.91	29754.27	40053.83	49781.18	208279.9	267101.8	330158	400538.3	480073.7	572197.5
0.14	10039.55	20648.6	30677.92	41297.2	51326.52	214745.4	275393.3	340406.9	412972	494976.4	589960
0.145	10337.66	21261.71	31588.83	42523.43	52850.54	221121.8	283570.5	350514.5	425234.3	509673.6	607477.5
0.15	10631.59	21866.25	32487	43732.5	54353.25	227409	291633.3	360480.8	437325	524165.3	624750
0.155	10921.35	22462.21	33372.43	44924.43	55834.64	233607	299581.7	370305.6	449244.3	538451.3	641777.5
0.16	11206.94	23049.6	34245.12	46099.2	57294.72	239715.8	307415.8	379989.1	460992	552531.8	658560

0.165	11488.37	23628.41	35105.07	47256.83	58733.48	245735.5	315135.5	389531.3	472568.3	566406.8	675097.5
0.17	11765.62	24198.65	35952.28	48397.3	60150.93	251666	322740.9	398932	483973	580076.2	691390
0.175	12038.71	24760.31	36786.75	49520.63	61547.06	257507.3	330231.8	408191.4	495206.3	593540.1	707437.5
0.18	12307.63	25313.4	37608.48	50626.8	62921.88	263259.4	337608.4	417309.5	506268	606798.4	723240
0.185	12572.37	25857.91	38417.47	51715.83	64275.38	268922.3	344870.7	426286.2	517158.3	619851.1	738797.5
0.19	12832.95	26393.85	39213.72	52787.7	65607.57	274496	352018.5	435121.5	527877	632698.3	754110
0.195	13089.36	26921.21	39997.23	53842.43	66918.44	279980.6	359052.1	443815.4	538424.3	645339.9	769177.5
0.2	13341.6	27440	40768	54880	68208	285376	365971.2	452368	548800	657776	784000
0.205	13589.67	27950.21	41526.03	55900.43	69476.24	290682.2	372776	460779.2	559004.3	670006.5	798577.5
0.21	13833.57	28451.85	42271.32	56903.7	70723.17	295899.2	379466.4	469049.1	569037	682031.5	812910
0.215	14073.3	28944.91	43003.87	57889.83	71948.78	301027.1	386042.4	477177.6	578898.3	693850.9	826997.5
0.22	14308.87	29429.4	43723.68	58858.8	73153.08	306065.8	392504.1	485164.7	588588	705464.8	840840
0.225	14540.26	29905.31	44430.75	59810.63	74336.06	311015.3	398851.4	493010.4	598106.3	716873.1	854437.5
0.23	14767.48	30372.65	45125.08	60745.3	75497.73	315875.6	405084.4	500714.8	607453	728075.8	867790
0.235	14990.54	30831.41	45806.67	61662.83	76638.08	320646.7	411203	508277.9	616628.3	739073	880897.5
0.24	15209.42	31281.6	46475.52	62563.2	77757.12	325328.6	417207.2	515699.5	625632	749864.6	893760
0.245	15424.14	31723.21	47131.63	63446.43	78854.84	329921.4	423097	522979.8	634464.3	760450.7	906377.5
0.25	15634.69	32156.25	47775	64312.5	79931.25	334425	428872.5	530118.8	643125	770831.3	918750

0.255	15841.07	32580.71	48405.63	65161.43	80986.34	338839.4	434533.6	537116.3	651614.3	781006.2	930877.5
0.26	16043.27	32996.6	49023.52	65993.2	82020.12	343164.6	440080.4	543972.5	659932	790975.6	942760
0.265	16241.31	33403.91	49628.67	66807.83	83032.58	347400.7	445512.8	550687.4	668078.3	800739.5	954397.5
0.27	16435.18	33802.65	50221.08	67605.3	84023.73	351547.6	450830.8	557260.8	676053	810297.8	965790
0.275	16624.88	34192.81	50800.75	68385.63	84993.56	355605.3	456034.4	563692.9	683856.3	819650.6	976937.5
0.28	16810.42	34574.4	51367.68	69148.8	85942.08	359573.8	461123.7	569983.7	691488	828797.8	987840
0.285	16991.78	34947.41	51921.87	69894.83	86869.28	363453.1	466098.6	576133.1	698948.3	837739.4	998497.5
0.29	17168.97	35311.85	52463.32	70623.7	87775.17	367243.2	470959.2	582141.1	706237	846475.5	1008910
0.295	17342	35667.71	52992.03	71335.43	88659.74	370944.2	475705.4	588007.7	713354.3	855006	1019078
0.3	17510.85	36015	53508	72030	89523	374556	480337.2	593733	720300	863331	1029000
0.305	17675.54	36353.71	54011.23	72707.43	90364.94	378078.6	484854.7	599316.9	727074.3	871450.4	1038678
0.31	17836.05	36683.85	54501.72	73367.7	91185.57	381512	489257.7	604759.5	733677	879364.3	1048110
0.315	17992.4	37005.41	54979.47	74010.83	91984.88	384856.3	493546.5	610060.7	740108.3	887072.6	1057298
0.32	18144.58	37318.4	55444.48	74636.8	92762.88	388111.4	497720.8	615220.5	746368	894575.4	1066240
0.325	18292.58	37622.81	55896.75	75245.63	93519.56	391277.3	501780.8	620238.9	752456.3	901872.6	1074938
0.33	18436.42	37918.65	56336.28	75837.3	94254.93	394354	505726.5	625116	758373	908964.2	1083390
0.335	18576.09	38205.91	56763.07	76411.83	94968.98	397341.5	509557.7	629851.8	764118.3	915850.3	1091598
0.34	18711.59	38484.6	57177.12	76969.2	95661.72	400239.8	513274.6	634446.1	769692	922530.8	1099560

0.345	18842.93	38754.71	57578.43	77509.43	96333.14	403049	516877.1	638899.1	775094.3	929005.8	1107278
0.35	18970.09	39016.25	57967	78032.5	96983.25	405769	520365.3	643210.8	780325	935275.3	1114750
0.355	19093.08	39269.21	58342.83	78538.43	97612.04	408399.8	523739.1	647381	785384.3	941339.1	1121978
0.36	19211.9	39513.6	58705.92	79027.2	98219.52	410941.4	526998.5	651409.9	790272	947197.4	1128960
0.365	19326.56	39749.41	59056.27	79498.83	98805.68	413393.9	530143.6	655297.5	794988.3	952850.2	1135698
0.37	19437.04	39976.65	59393.88	79953.3	99370.53	415757.2	533174.3	659043.6	799533	958297.4	1142190
0.375	19543.36	40195.31	59718.75	80390.63	99914.06	418031.3	536090.6	662648.4	803906.3	963539.1	1148438
0.38	19645.51	40405.4	60030.88	80810.8	100436.3	420216.2	538892.6	666111.9	808108	968575.2	1154440
0.385	19743.48	40606.91	60330.27	81213.83	100937.2	422311.9	541580.2	669434	812138.3	973405.7	1160198
0.39	19837.29	40799.85	60616.92	81599.7	101416.8	424318.4	544153.4	672614.7	815997	978030.7	1165710
0.395	19926.93	40984.21	60890.83	81968.43	101875	426235.8	546612.3	675654	819684.3	982450.1	1170978
0.4	20012.4	41160	61152	82320	102312	428064	548956.8	678552	823200	986664	1176000
0.405	20093.7	41327.21	61400.43	82654.43	102727.6	429803	551186.9	681308.6	826544.3	990672.3	1180778
0.41	20170.83	41485.85	61636.12	82971.7	103122	431452.8	553302.7	683923.9	829717	994475.1	1185310
0.415	20243.79	41635.91	61859.07	83271.83	103495	433013.5	555304.1	686397.8	832718.3	998072.3	1189598
0.42	20312.59	41777.4	62069.28	83554.8	103846.7	434485	557191.2	688730.3	835548	1001464	1193640
0.425	20377.21	41910.31	62266.75	83820.63	104177.1	435867.3	558963.8	690921.4	838206.3	1004650	1197438
0.43	20437.66	42034.65	62451.48	84069.3	104486.1	437160.4	560622.1	692971.2	840693	1007631	1200990
0.435	20493.95	42150.41	62623.47	84300.83	104773.9	438364.3	562166.1	694879.7	843008.3	1010406	1204298
0.44	20546.06	42257.6	62782.72	84515.2	105040.3	439479	563595.6	696646.7	845152	1012975	1207360
0.445	20594.01	42356.21	62929.23	84712.43	105285.4	440504.6	564910.9	698272.4	847124.3	1015339	1210178
0.45	20637.79	42446.25	63063	84892.5	105509.3	441441	566111.7	699756.8	848925	1017497	1212750
0.455	20677.4	42527.71	63184.03	85055.43	105711.7	442288.2	567198.2	701099.7	850554.3	1019450	1215078
0.46	20712.83	42600.6	63292.32	85201.2	105892.9	443046.2	568170.3	702301.3	852012	1021197	1217160
0.465	20744.1	42664.91	63387.87	85329.83	106052.8	443715.1	569028	703361.6	853298.3	1022739	1218998
0.47	20771.2	42720.65	63470.68	85441.3	106191.3	444294.8	569771.4	704280.4	854413	1024075	1220590
0.475	20794.13	42767.81	63540.75	85535.63	106308.6	444785.3	570400.4	705057.9	855356.3	1025206	1221938
0.48	20812.9	42806.4	63598.08	85612.8	106404.5	445186.6	570915.1	705694.1	856128	1026131	1223040
0.485	20827.49	42836.41	63642.67	85672.83	106479.1	445498.7	571315.4	706188.9	856728.3	1026850	1223898
0.49	20837.91	42857.85	63674.52	85715.7	106532.4	445721.6	571601.3	706542.3	857157	1027364	1224510
0.495	20844.17	42870.71	63693.63	85741.43	106564.3	445855.4	571772.8	706754.3	857414.3	1027672	1224878
0.5	387000	42875	63700	85750	106575	445900	571830	706825	857500	1027775	1225000

Fig 1: Sample curve for the relationship between velocity component against vertical distances from bottom surface.

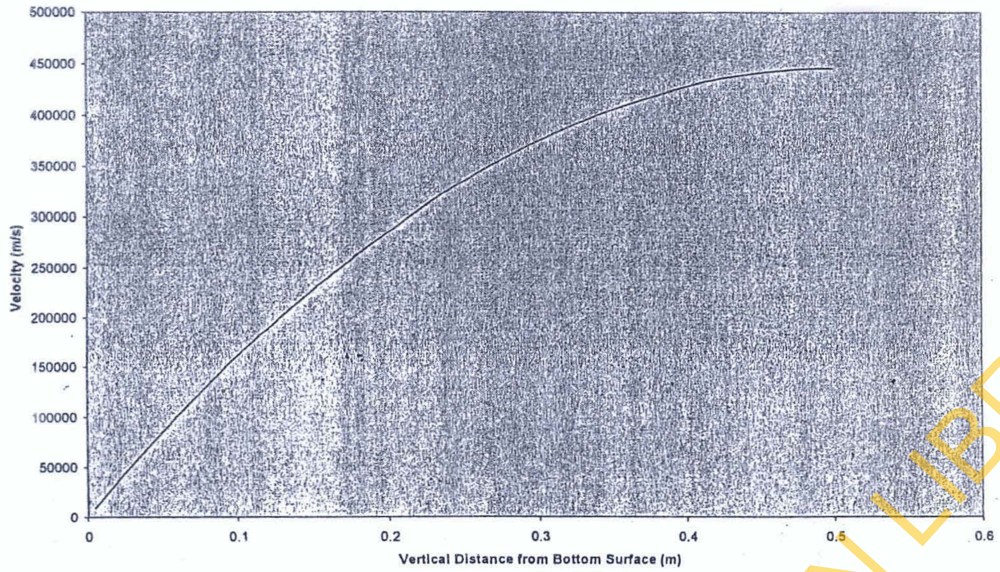

Fig 2: Velocity components against Vertical distance at different slopes.

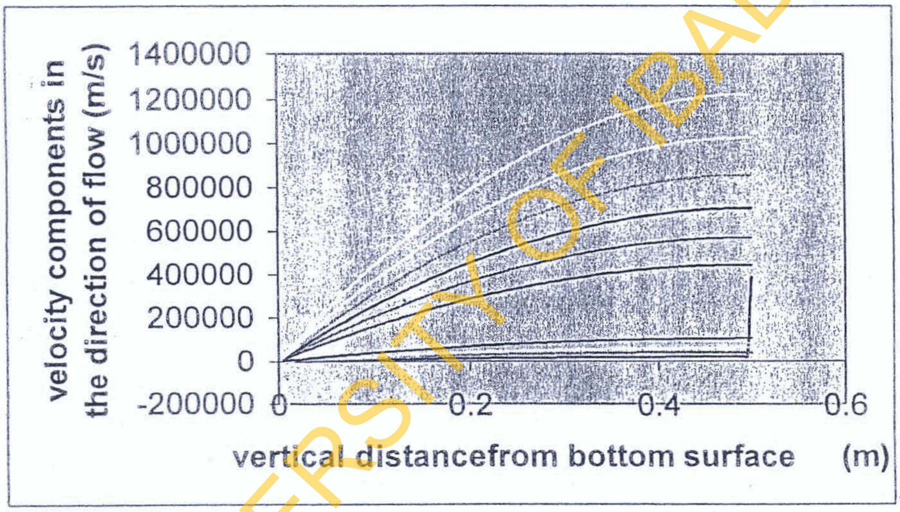

Table 2 : Velocity at Y=0.05 as slope changes

S/N	Y =y (m)	V (m/s)	So
1	0.05	208.4625	0.017
2	0.05	429.19	0.035
3	0.05	637.65	0.052
4	0.05	858.375	0.07
5	0.05	1066.838	0.087
6	0.05	4414.5	0.36
7	0.05	5714.325	0.466
8	0.05	7075.463	0.577
9	0.05	8583.75	0.7
19	0.05	10288.24	0.839
11	0.05	12262.5	1

Fig. 3: Slope of bottom surface against.